Pharm Res (2012) 29:2468–2476
DOI 10.1007/s11095-012-0776-7

RESEARCH PAPER

Discrepancies in the P-glycoprotein-Mediated Transport of ^{18}F-MPPF: A Pharmacokinetic Study in Mice and Non-human Primates

Nicolas Tournier • Salvatore Cisternino • Marie-Anne Peyronneau • Sébastien Goutal • Frédéric Dolle • Jean-Michel Scherrmann • Michel Bottlaender • Wadad Saba • Héric Valette

Received: 7 February 2012 / Accepted: 9 May 2012 / Published online: 30 May 2012

ABSTRACT

Purpose Several *in vivo* studies have found that the 5-HT$_{1A}$ PET radioligand ^{18}F-MPPF is a substrate of rodent P-glycoprotein (P-gp). However, *in vitro* assays suggest that MPPF is not a substrate of human P-gp. We have now tested the influence of inhibiting P-gp on the brain kinetics of ^{18}F-MPPF in mice and non-human primates.

Methods We measured the peripheral kinetics (arterial input function, metabolism, free fraction in plasma (f_P)) during ^{18}F-MPPF brain PET scanning in baboons with or without cyclosporine A (CsA) infusion. We measured ^{3}H-MPPF transport at the mouse BBB using *in situ* brain perfusion in P-gp/Bcrp deficient mice and after inhibiting P-gp with PSC833.

Results There was an unexpected 1.9-fold increase in brain area under the curve in CsA-treated baboons (n=4), with no change in radiometabolite-corrected arterial input. However, total volume of distribution corrected for f_P (V_T/f_P) remained unchanged. *In situ* brain perfusion showed that P-gp restricted the permeability of the mouse BBB to ^{3}H-MPPF while Bcrp did not.

Conclusion These and previous *in vitro* results suggest that P-gp may not influence the permeability of human BBB to ^{18}F-MPPF. However, CsA treatment increased ^{18}F-MPPF free fraction, which is responsible for a misleading, P-gp unrelated enhanced brain uptake.

N. Tournier (✉) • M.-A. Peyronneau • S. Goutal • F. Dolle •
M. Bottlaender • W. Saba • H. Valette
CEA, I2BM, Service Hospitalier Frédéric Joliot
Orsay 91401, France
e-mail: nicolas.tournier@cea.fr

S. Cisternino • J.-M. Scherrmann
INSERM U705, CNRS UMR8206, Faculté de Pharmacie
Université Paris Descartes
Sorbonne Paris Cité, Université Paris Diderot
Paris, France

KEY WORDS blood–brain barrier · plasma protein binding · positron emission tomography · P-glycoprotein · ^{18}F-MPPF

ABBREVIATIONS

ABC	ATP–binding cassette
AUC	area under the curve
BBB	blood–brain barrier
BCRP	breast cancer resistance protein
CNS	central nervous system
CsA	cyclosporine A
f_P	free fraction (unbound) in plasma
HPLC	high performance liquid chromatography
MDCK	Madin-Darby canine kidney cells
MPPF	4-fluoro-*N*-{2-[4-(2-methoxy-phenyl)-piperazin-1-yl]-ethyl}-*N*-pyridin-2-yl-benzamide
PET	positron emission tomography
PK	pharmacokinetic
P-gp	P-glycoprotein
VOI	volume of interest
V_T	total distribution volume

INTRODUCTION

Recent studies on drug transporters have added a new layer of complexity to our understanding of drug pharmacokinetics (PK; (1)). Several years ago, passive diffusion was believed to be the only process by which xenobiotics cross body membranes, including the blood–brain barrier (BBB). Drugs were developed for CNS activity according to their physicochemical specifications and variations in their clinical effect were ascribed mainly to their pharmacological target or metabolic pathways (2). However, the brain flux of some drugs and radiotracers was shown to be partly controlled by the activity

of transporters like the ATP–binding cassette (ABC) proteins, which includes at least the P-glycoprotein (P-gp, ABCB1) and the breast cancer resistance protein (BCRP, ABCG2). These unidirectional efflux transporters, which are present only on the luminal side of the brain endothelial cells that form the BBB, are involved in reducing the entry of drugs into the brain parenchyma, at least in humans and rodents (3).

ABC-mediated transport can be pharmacologically modulated with inhibitors or inducers which can alter the PK of ABC-substrates (4). This transport activity may also account for variations in the kinetics of PET tracers and influences brain imaging and quantification. Several studies have shown that the abundance and functionality of P-gp is affected by pathophysiological states such as neuropsychiatric and neurodegenerative disorders like Alzheimer disease and epilepsy (5–7). Thus, it is now agreed that the transport of tracers by P-gp and BCRP should be documented, as is recommended for therapeutic agents (8,9). The 5-HT$_{1A}$ serotoninergic receptor antagonist ^{18}F-MPPF (4-^{18}F-fluoro-*N*-{2-[4-(2-methoxy-phenyl)-piperazin-1-yl]-ethyl}-*N*-pyridin-2-yl-benzamide) is a useful ^{18}fluorine-radiolabeled alternative to the structurally related ^{11}C-WAY100635 and ^{11}C-*R*WAY (10). However, several *in vivo* PK studies have shown that the uptake of ^{18}F-MPPF by the rodent brain is significantly influenced by P-gp (11–16). Based on these results, ^{18}F-MPPF was used as a probe in PET studies on P-gp function in rodents, suggesting its possible use to evaluate pharmaco-resistance in patients suffering from seizure disorders (14,17). The counterpart is the likely troublesome contribution of P-gp to ^{18}F-MPPF kinetics, which may affect the interpretation of PET results when studying 5-HT$_{1A}$ receptors. Our recent *in vitro* study showed that MPPF is not a substrate of human P-gp, which raises the question of variations between species as well as the clinical impact of P-gp on ^{18}F-MPPF transport (18). Others have also described significant differences in the transport and spectra of P-gp substrates or inhibitors between the human and rodent isoforms (19,20). However, preliminary results obtained in a clinical study indicate that the P-gp inhibitor cyclosporine A significantly increases ^{18}F-MPPF brain uptake. This study on ten patients suffering from temporal lobe epilepsy who underwent paired ^{18}F-MPPF PET scans with and without CsA infusion (2.5 mg/kg/h) showed a significant increase (14%) in ^{18}F-MPPF binding potential in most brain regions, regardless of their involvement in seizure generation or propagation (17).

We have now attempted to clarify these discrepancies using complementary *in vitro* and *in vivo* techniques to evaluate the influence of P-gp on ^{18}F-MPPF brain kinetics in mice and non-human primates. We used PET imaging to assess the effects of CsA on the brain kinetics of ^{18}F-MPPF in baboons, as well as any simultaneous changes in ^{18}F-MPPF peripheral metabolism and binding to plasma proteins. Human-specific *in vitro* transport assays were also used to test the transport of both ^{18}F-MPPF and its main radiometabolite by the human isoform of P-gp. We used *in situ* brain perfusion rather than conventional systemic PK to simplify the analysis of the brain kinetics in mice: this method assessed the intrinsic MPPF transport at the mouse BBB and the effects of P-gp modulation without influence of peripheral metabolism, systemic elimination and protein binding.

MATERIALS AND METHODS

Chemicals

PSC833 (valspodar) was a gift from Novartis (Switzerland). CsA was administered using the Sandimmun® formulation (Novartis). All other chemicals were analytical grade.

Radiochemicals

^{3}H-MPPF, ^{3}H-prazosin and ^{14}C-sucrose were purchased from Perkin-Elmer (France). Ready-to-inject, >99% radiochemically pure ^{18}F-MPPF was prepared from cyclotron-produced ^{18}F-fluoride (Cyclone-18/9 cyclotron, IBA, Belgium) based on published standard conditions (21) consisting of nitro-for-fluorine nucleophilic aromatic substitution of the corresponding nitro-precursor for labelling (4-nitro-N-{2-[4-(2-methoxy-phenyl)-piperazin-1-yl]-ethyl}-N-pyridin-2-yl-benzamide (ABX, Germany) using a TRACERLab® FX-FN synthesizer (GEMS, France).

Animals

All procedures using animals were in strict accordance with the recommendations of the European Community (86/609/CEE) and the French National Committee (law 87/848) for the care and use of laboratory animals.

PET studies were carried out on two adult *Papio anubis* baboons weighing 18 and 20 kg. All animals were housed in a controlled environment (22 ± 3°C; 55% ± 10% relative humidity) and a 12-h dark–light cycle, with access to food and tap water *ad libitum*. Adult male Fvb mice (30–40 g, 7–11 weeks old) were obtained from Janvier (Genest, France). The triple knockout (KO) mouse strain Mdr1a/1b;Bcrp$^{(-/-;\ -/-)}$, also called P-gp/Bcrp$^{(-/-)}$, was bred in-house from progenitors obtained from the laboratory of Dr. Alfred H. Schinkel (The Netherlands Cancer Institute, The Netherlands). This strain was derived from Fvb mice.

PET Study in Baboons

PET Imaging

We studied the brain distribution of ^{18}F-MPPF in adult baboons. They were anaesthetized and PET data were

acquired as previously described (22). Each baboon underwent two control and two CsA-treated PET scans. Experiments were performed at least two weeks apart on an HR + tomograph (Siemens, Knoxville TS, USA). They were injected i.v with 296 to 370 MBq ^{18}F-MPPF and images were collected for at least 120 min. Blood samples were taken from a femoral artery at designated times. The P-gp inhibitor CsA (15 mg/kg/h i.v.) (n=4) was infused for 30 min before and during the PET experiment.

PET Data Analysis

Regional time activity curves were generated by calculating the mean radioactivity in selected volumes of interests (VOIs): hippocampus, whole brain hemispheres and cerebellum, correcting them for ^{18}F decay and injected radioactivity. PET data are given as calculated areas under the curve (AUC) in each VOI. Receptor-radioligand binding parameters were modelled from time-activity data by the Logan graphical method (23) using the metabolite-corrected plasma input function. This method was used to estimate the total distribution volume (V_T) of the ligand (PMOD® software).

Arterial Radiometabolite Corrected Input Function

Arterial plasma samples were deproteinated with acetonitrile and injected onto the UV/radioactive HPLC system. ^{18}F-MPPF and its radiometabolite(s) were separated using a SunFire® C18 5 µm 10×250 mm semi-preparative column at 35°C (Waters, France). The mobile phases were 0.1% trifluoroacetic acid in water (A) and 0.1% trifluoroacetic acid in acetonitrile (B). Solutes were eluted (5 ml/min) with a gradient of 10 to 55% B (and A from 90 to 45%) over 13 min (UV detection, 275 nm).

Determination of Free ^{18}F-MPPF in Plasma

The fraction of ^{18}F-MPPF in baboon plasma samples that was not bound to plasma protein was measured before and during CsA infusion. Standard amounts of ^{18}F-MPPF solution (~50 kBq) were added to 200 µl plasma samples. These solutions were applied to Microcon® filtration devices containing a YM-10 membrane (Millipore, France) and the devices were centrifuged for 20 min at 10,000 g (Biofuge Primo® R, Heraeus, France). The ^{18}F activities in the resulting ultrafiltrate (~100 µL, C_{FP}) and a sample of plasma (C_P) were counted. The free fraction (f_P) of ^{18}F-MPPF was calculated as: $f_P = C_{FP}/C_P$.

P-gp-Mediated Transport of ^{18}F-MPPF Radiometabolite

Data from a reliable *in vitro* model indicate that MPPF itself cannot be considered to be a substrate of human P-gp (18). We therefore assayed the transport of the main radiometabolite of ^{18}F-MPPF by P-gp using the concentration equilibrium assay. Arterial baboon plasma (without CsA) sampled 30 min after ^{18}F-MPPF injection was tested using the concentration equilibrium assay. Radio-HPLC analysis of this sample showed that ~80% of the radioactivity was due to a single radiometabolite at that time, whereas the parent compound accounted for ~20% of the radioactivity (Fig. 1). MDCK-hMDR1 cells (a gift from Dr A.H. Schinkel) cultured in Transwell® monolayers were used to assay transport as previously described (18,24). Briefly, the culture medium was removed and cells were pre-incubated for 1 h with incubation buffer in both the apical (A, 0.5 mL) and basolateral (B, 1.5 mL) compartments, with or without a P-gp inhibitor (5 µM PSC833). This pre-incubation buffer was then removed and replaced in both compartments by the same buffer containing 10% (v/v) of the tested plasma, with or without the inhibitor. The incubation solution also contained 3.7 kBq/mL of the P-gp substrate ^{3}H-prazosin, as an internal positive control of model function. We also assayed the P-gp mediated transport of ^{18}F-MPPF (~10 kBq/mL). The assay systems were incubated at 37°C for 3 h and the radioactivity in each compartment was determined. Tritium radioactivity from ^{3}H-prazosin was measured two days later, to allow the fluorine-18 to decay. Polarized transport was identified when the concentration in A was significantly greater than that in B. The specificity of any polarized transport was determined by the effect of the P-gp inhibitor.

In Situ Brain Perfusion in Mice

Surgery and Perfusion

In situ brain perfusion was performed as previously described (25). The intrinsic transport rate or brain clearance (K_{in}, n=4) at the luminal BBB membrane for ^{3}H-MPPF was measured in wild-type mice and compared to the data obtained in wild-type mice after inhibition of P-gp with 3 µM PSC833 and in P-gp/Bcrp$^{(-/-)}$ mice. Each mouse was perfused with protein-free Krebs carbonate-buffered physiological saline containing a known concentration of ^{3}H-MPPF (11 kBq/ml), and the vascular integrity marker ^{14}C-sucrose (3.7 kBq/ml), with or without the P-gp inhibitor PSC833 (3 µM). This perfusion fluid replaced all the blood in the right brain vasculature. The brains were perfused using an infusion pump (flow rate: 2.5 ml/min) and the mouse was decapitated after 60 s of perfusion.

Calculation of BBB Transport Parameters

The intrinsic BBB parameters of ^{3}H-MPPF transport were calculated according to previous report (25). The brain vascular volume was calculated using the distribution of ^{14}C-sucrose, which does not measurably cross the BBB in a short time. The distribution volume of ^{14}C-sucrose was used to check

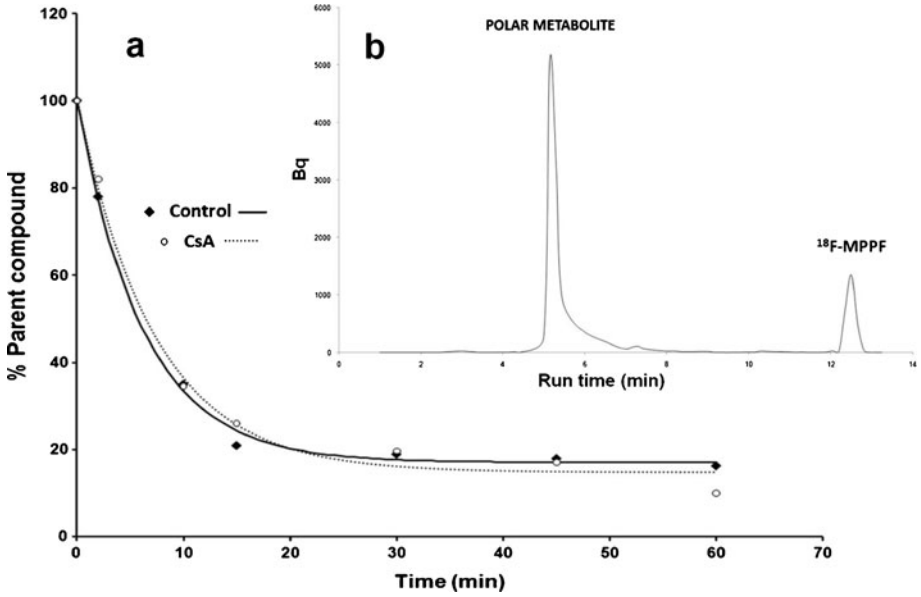

Fig. 1 HPLC analysis of the ^{18}F-MPPF input function. (**a**) Mean fraction of parent compound in plasma *versus* time and fitted curves after ^{18}F-MPPF injection of controls (n=4, closed symbol, *black line*) and CsA-treated baboons (n=4; opened symbol, *dotted line*). Data are expressed as percentages of the total radiolabeled peak areas determined using HPLC radiochromatography. (**b**) Representative radioactive HPLC chromatogram of baboon plasma obtained 30 min after injecting ^{18}F-MPPF.

the BBB integrity and enabled us to correct ^{3}H-MPPF brain activity from the vascular content. The apparent distribution volume of ^{3}H-MPPF (V_{brain}; µl/g) and its transport rate or brain clearance were calculated from the tritium radioactivity in the right hemisphere ($K_{in}=V_{brain}/60s$; µl/s/g).

Statistical Analysis

The PET data obtained for baboons 1 and 2 were compared using a two-way (baboon and treatment) analysis of variance to assess the effect of CsA treatment. The interaction term (baboon) was not significant for tested values. The mouse groups used for *in situ* brain perfusion were compared using Student's *t*-test, as were the *in vitro* data obtained with the concentration equilibrium assay. The tests were two-tailed and significance was set at $p<0.05$.

RESULTS

PET Study in Baboons

CsA perfusion had no effect on the plasma kinetics of ^{18}F-MPPF evaluated as mean $AUC_{0\text{-}80}$ (Figs. 2 and 3). Therefore, CsA did not influence the peripheral clearance of ^{18}F-MPPF and thus the exposure of the brain to this tracer. The metabolite study showed that CsA did not alter the percentage of plasma parent compound over time (Fig. 1). Radio-HPLC revealed that similar concentrations *versus* time of a single radiometabolite were present in the plasma of controls and CsA-treated baboons (Fig. 1). The unbound ^{18}F-MPPF in the plasma of control baboons (without CsA) was 6.0±0.4% in baboon 1 and 10.3±1.0% in baboon 2. CsA perfusion led to an ~1.9-fold increases in f_P (Table I). The *in vitro* concentration equilibrium assay showed that neither ^{18}F-MPPF nor its main radiometabolite are substrates of human P-gp (Fig. 4).

The PET data revealed that the brains of CsA-treated baboons took up significantly more radioactivity than did those of controls (Figs. 2 and 3). V_T was increased by similar magnitudes in all the VOIs of the CsA-treated baboons, independently of the 5-HT_{1A} target density. Thus, CsA treatment seemed to improve the crossing of the BBB by the tracer. But CsA treatment produced no change in the V_T corrected for f_P (V_T/f_P) in any of the VOIs, suggesting that the increase in V_T was related only to the increase in the free fraction of tracer in the plasma (Fig. 5, Table I).

In Situ Brain Perfusion in Mice

The intrinsic brain transport of ^{3}H-MPPF in wild-type mice was 19.8±2.0 µl/s/g. The brain clearance of diazepam (a flow marker) measured in the same conditions was 42.3 µl/s/g (25). This indicates that the brain took up 46.8% of the ^{3}H-MPPF. The brain transport (K_{in}) of ^{3}H-MPPF by wild-type mice perfused with PSC833 was 1.5-times greater than in control wild-type mice (Fig. 6). Similarly, the brains of P-gp/Bcrp deficient mice took up 1.5-times more ^{3}H-MPPF than did those of control wild-type mice (Fig. 6). Thus, MPPF is a substrate of mouse P-gp. Moreover, the lack of any difference in the uptake of MPPF by the brains of mice after inhibition of P-gp with PSC833 and those of P-gp/Bcrp KO mice suggests that Bcrp is not involved in ^{3}H-MPPF transport.

DISCUSSION

Great efforts have been made to develop PET radioligands that are selective for the 5-HT_{1A} receptor because of the implication

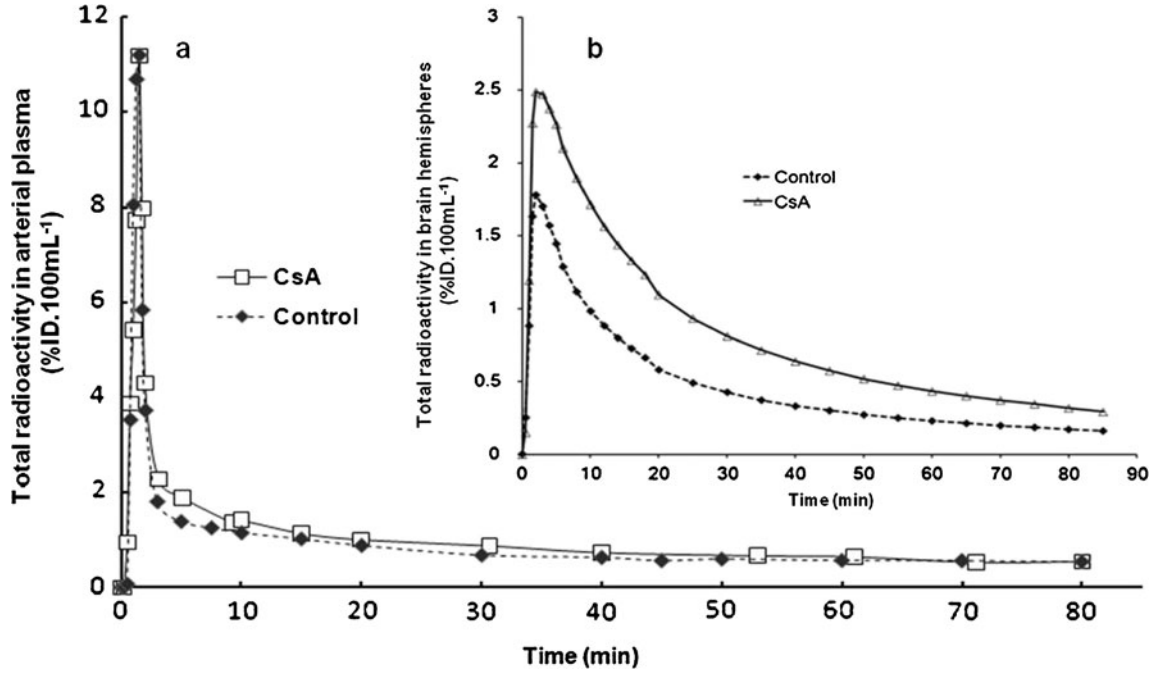

Fig. 2 Radioactivity in arterial blood plasma (**a**) and PET time-activity curve in whole brain hemispheres (**b**) measured after injecting ^{18}F-MPPF into a control baboon (*black symbols*) and following CsA infusion (*open symbols*).

of these receptors in neuropsychiatric diseases. ^{18}F-MPPF appears to be a useful fluorine-18 radiolabeled alternative to ^{11}C-[carbonyl]-WAY-100635 (26). Unfortunately, these compounds were identified as P-gp substrates in rodents (15,16), which complicates the interpretation of PET data. However, data from an *in vitro* study showed that MPPF is not a substrate of human P-gp (18), suggesting confounding species difference. Surprisingly, the results of a clinical study revealed that CsA significantly increased the brain uptake of ^{18}F-MPPF (17). Pharmacological agents like CsA can affect many systemic PK factors and produce drug-tracer interactions that are not related to P-gp. These, in turn, could increase the amount of drug in the brain independently of the capacity of the tracer/drug to interact with P-gp. We studied the effect of the prototypical P-gp inhibitor CsA on ^{18}F-MPPF PK transport into the brains of baboons to clarify these discrepancies. CsA was the P-gp inhibitors selected because it is readily available and it enabled us to allow compare directly our findings with published CsA studies (11,12,15–17). The CsA dosing protocol (15 mg/kg/h) was based on previous studies showing that it effectively inhibited P-gp at the monkey BBB when ^{11}C-(*R*)-verapamil was used as the PET probe (27). We used the same CsA challenge for ^{11}C-*N*-desmethyl-loperamide, which suitably inhibited P-gp at the baboon BBB (data not shown).

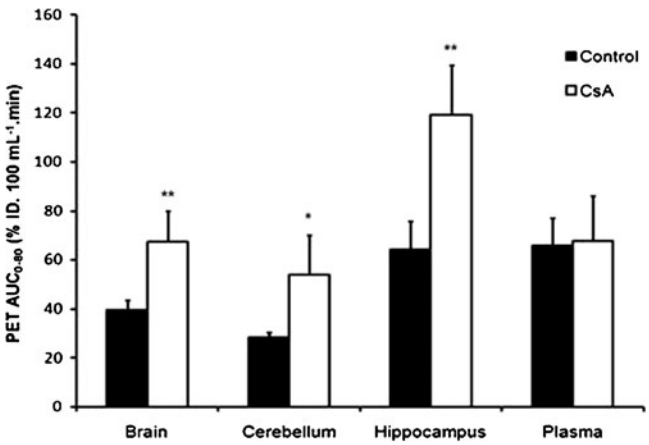

Fig. 3 Radioactivity in brain tissues and arterial blood plasma expressed as the AUC from 0 to 80 min post-injection of ^{18}F-MPPF in control baboons (filled bars) and following CsA infusion (open bars). $n=4$ for each condition. (*=$p<0.05$; **=$p<0.01$).

CsA can target components of the input function like the tracer peripheral distribution volume and its biotransformation. CsA interacts with CYP3A (28), which could modify ^{18}F-MPPF metabolism (29). Laćan *et al.* (11) found that CsA had no effect on either the ^{18}F-MPPF input function or its metabolism in rodents, while the brain uptake increased. They concluded that there is no peripheral interaction between CsA and ^{18}F-MPPF kinetics and that the increased ^{18}F-MPPF uptake by the brain is due solely to inhibition of the P-gp at the BBB. And tariquidar, a third-generation P-gp inhibitor with no effect on cytochrome P450 activity (30), also significantly increased the uptake of ^{18}F-MPPF by the brains of rodents (13,14). We used *in situ* brain perfusion to avoid the numerous other PK confounding factors arising from the peripheral

Table I Distribution volumes (V_T) Obtained for ^{18}F-MPPF in Baboon Brain Hemispheres, Hippocampus and Cerebellum with or without Cyclosporine A (CsA), Estimated by the Logan Graphical Method Using the Metabolite-Corrected Input Function. V_T Corrected for ^{18}F-MPPF Free Fraction in Plasma (V_T/f_P) are Also Showed

		f_P	V_T			V_T/f_P		
			Brain	Cerebellum	Hippocampus	Brain	Cerebellum	Hippocampus
Baboon 1	Control	0.106	1.57	1.26	2.80	27.5	22.1	49.1
		0.101	1.51	0.90	2.52	24	14.3	40.2
	CsA	0.196	2.68	1.88	4.70	24.8	17.4	43.5
		0.177	2.72	1.78	4.50	23.9	15.6	39.5
Baboon 2	Control	0.057	2.39	1.54	4.24	22.5	14.5	40.0
		0.063	2.24	1.44	3.01	22.2	14.3	29.8
	CsA	0.108	3.98	2.98	7.78	20.3	15.2	39.7
		0.114	4.09	2.50	5.93	23.1	14.1	33.5

metabolism and clearance of the tracer. This method is a valuable tool for studying transport mechanisms at the BBB and intrinsic permeability parameters. It provides results that are independent of peripheral components because the brain circulation is isolated from the rest of the body (25). Our results confirm that MPPF is a substrate of murine P-gp. The PK study of the input function in baboons revealed that neither the total radioactivity nor the concentration of the parent compound in the blood plasma was affected by CsA (Figs. 1, 2 and 3). An *in vitro* study on human hepatocytes detected two major radiometabolites of MPPF (29): a hydroxyphenolic derivative, and ^{18}F-fluorobenzoic acid, very little of which is taken up by the brain (31). Based on these results, we

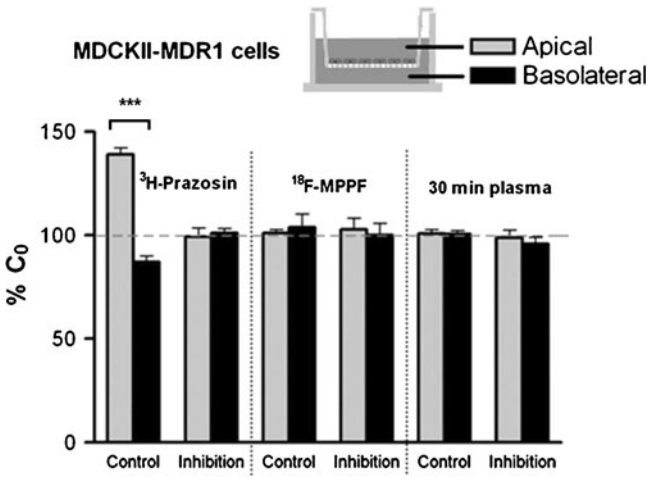

Fig. 4 *In vitro* study of the P-gp mediated transport of ^{18}F-MPPF and its main metabolite using the concentration equilibrium assay on MDCKII-hMDR1 cells. Results are expressed as percentages ± S.D ($n=6$) of initial concentration (C_0) obtained in apical (A, clear column) and basolateral (B, black column) compartments at the end of the assay with and without the P-gp inhibitor 5 μM PSC833. The transport of the main radiometabolite of ^{18}F-MPPF was studied using a plasma sample containing ~80% of this compound according to radio-HPLC analysis ("30 min plasma" columns). The P-gp substrate ^{3}H-prazosin was used as a positive control. Polarized transport was identified when the concentration in A was significantly greater than that in B. Any polarized transport had to be abolished by PSC833 to ensure its specificity (***=$p<0.001$).

can consider that ^{18}F-MPPF is rapidly and preferentially metabolized to a hydroxylated radiometabolite, as there was no detectable ^{18}F-fluorobenzoic acid in the plasma (HPLC data not shown). Studies on rodents showed that ^{18}F-MPPF radiometabolite(s), more polar, do not cross the BBB as parent ^{18}F-MPPF accounted for more than 95% of the total radioactivity in brain tissue despite its extensive peripheral metabolism (32,33). This is why the ^{18}F-MPPF input function used for PK modeling in humans considers only the parent ^{18}F-MPPF to develop an adequate model of ^{18}F-MPPF brain kinetics (34). The Logan method used in this work using metabolite-corrected arterial plasma input has been successfully used to assess the V_T and has shown excellent fits in preliminary studies with ^{18}F-MPPF (35). We showed that the retention time and the proportion of the main radiometabolite measured by radio-HPLC were essentially the same with and without CsA (Fig. 1). Thus, CsA is not likely to alter the metabolism of ^{18}F-MPPF or to induce the production of a radiometabolite that could more efficiently cross the BBB. Another explanation is that the BBB permeability of this radiometabolite could be influenced by a P-gp mediated efflux (as is the case for buprenorphine and carbamezepine and their respective metabolite norbuprenorphine (36) and carbamazepine-10,11-epoxide (37)). This could be true for ^{18}F-MPPF, since the radiometabolite identified in plasma samples accounted for ~80% of the total radioactivity 30 min after injection (Fig. 1). However, neither the ^{18}F-MPPF radiometabolite produced *in vivo* nor intact ^{18}F-MPPF was transported by P-gp *in vitro*. The ^{18}F-MPPF input function can, therefore, be described by the radioactivity of the parent ^{18}F-MPPF in the plasma in both the absence and presence of P-gp inhibition.

It is now accepted that only the free fraction of a drug can cross membranes and the BBB (3,38). Clinical studies showed that a large fraction of injected ^{18}F-MPPF (~89%) is bound to plasma proteins. We obtained similar results in monkeys. Less of the radiolabeled metabolite of ^{18}F-MPPF is bound to human plasma proteins (~65%). This is not surprising because this metabolite is more hydrophilic than the parent compound (39). This suggests that the brain uptake of this metabolite is

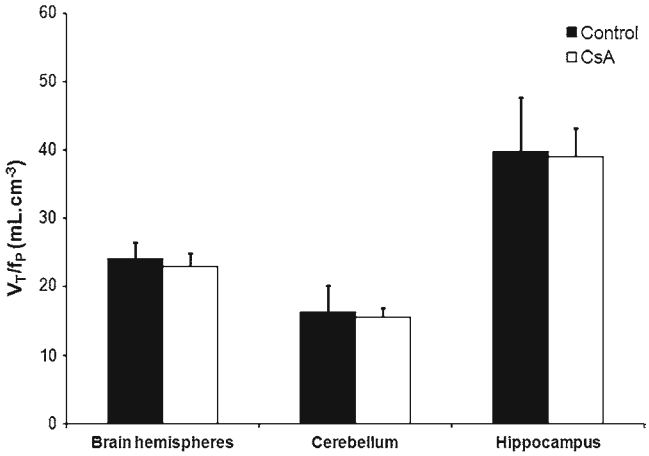

Fig. 5 Total distribution volumes (V_T) of ^{18}F-MPPF in brain hemispheres, hippocampus and cerebellum estimated by the Logan graphical method corrected for the free fraction of ^{18}F-MPPF measured in plasma (f_P) without (*black bars*), or with (*open bars*) CsA treatment. Data are presented as V_T/f_P (ml.cm^{-3}) ± S.D, n=4 in each condition.

not limited by its binding to proteins. CsA was shown to bind to plasma proteins and to displace several compounds from their plasma protein binding sites (40). This will increase the free fraction of a tracer and thus, its brain uptake (41). CsA treatment increased the ^{18}F-MPPF f_p in baboons ~2-fold. But the V_T corrected for f_P (V_T/f_P) in controls and CsA-treated animals were not significantly different, regardless of the 5-HT_{1A} receptor density (Fig. 5, Table I). This suggests that the increased uptake of ^{18}F-MPPF by the brain induced by CsA is attributable solely to its displacement from plasma proteins. Such a significant drug-tracer interaction may have influenced the systemic PK of ^{18}F-MPPF, with enhanced metabolic clearance of the tracer. However, CsA had no detectable influence on either the total radioactivity or the metabolite-corrected input function in our experimental conditions (Figs. 1, 2 and 3). Previous studies have reported that CsA increases the ^{11}C-*R*WAY f_p in rats (41). Tariquidar, another P-gp inhibitor used in monkeys, also increased ^{11}C-*R*WAY f_p

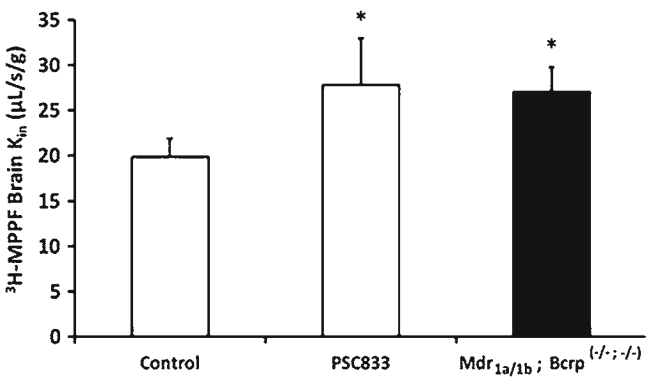

Fig. 6 ^{3}H-MPPF brain transport (K_{in}, n=4) measured by *in situ* brain perfusion in wild-type Fvb mice (white columns) with or without co-perfusion of PSC833 (3 µM), and in P-gp/Bcrp deficient mice (black column) (*=$p < 0.05$).

and this was also correlated with an increase in brain uptake, but with no significant influence on systemic PK (42). We know of no report describing the same effect of P-gp inhibitors on ^{18}F-MPPF brain kinetics. However, it is unlikely that there are any differences in the binding of ^{18}F-MPPF to plasma proteins in wild-type and KO strain, and the brain uptake of ^{18}F-MPPF measured in Mdr1a/1b$^{(-/-)}$ mice was 2–3 times greater than in wild-type mice, with no significant difference in the plasma radioactivity (12). The *in situ* brain perfusion technique allowed us to rule out any influence of plasma protein binding because the brain perfusate did not contain proteins. We can therefore compare the data obtained using pharmacological inhibition of the transporter and physical disruption. The brain transport rate of ^{3}H-MPPF was 1.5-fold higher in mice treated with the specific P-gp inhibitor PSC833 and in P-gp/Bcrp deficient mice. This confirms the influence of inhibiting P-gp on the uptake of ^{3}H-MPPF by the brains of rodents and its specificity toward Bcrp (Fig. 6).

Differences in the ABC substrates of human and rodent P-gp isoforms indicate that a careful check is needed before any further clinical use of a PET ligand as P-gp probe (19,43). For example, the properties of the PET ligand ^{11}C-*R*WAY as a P-gp substrate were characterized in rodents (41), but not in monkeys (42). We were unable to show any P-gp-mediated transport of MPPF using two widely used, sensitive, human-specific *in vitro* transport assays (18) that are recommended for use in drug development (9). *In vitro* assays using P-gp over-expressing cells such as those described here can detect the transport of weak P-gp substrates with exquisite sensitivity (24) and limit any bias encountered during *in vivo* studies. ^{18}F-MPPF should be tested on Mdr1-transfected cells from both mice and monkeys to identify the differences in its substrate status in the two species. An extensive study by Takeushi *et al.* (19) compared the efflux ratios of several P-gp substrates and found a good correlation between the MDR1 efflux for humans and monkeys, and a poor correlation between human MDR1 and mouse Mdr1a efflux. This result is supported that the amino-acid compositions of human P-gp and those of Rhesus monkeys (93% and chimpanzees (97%) are very much more similar than are those of rats (85%) and mice (87%) (43). Clearly, these data for ^{18}F-MPPF indicate that it is important to study carefully the input function, metabolism and plasma protein binding of a PET probe before reaching any conclusion about possible specific P-gp effects (44).

CONCLUSION

Despite evidence for the P-gp mediated transport of ^{18}F-MPPF at the rodent BBB, our *in vitro* data indicate that ^{18}F-MPPF is not a substrate of human P-gp. The effect of the P-gp inhibitor CsA on the brain transport of ^{18}F-MPPF in a non-human primate is related to an increase in the free fraction of

tracer in the plasma. Thus, it is unlikely that the kinetics of ^{18}F-MPPF brain transport and distribution are affected by P-gp activity in humans.

ACKNOWLEDGMENTS AND DISCLOSURES

We thank Dr. Alfred H. Schinkel (The Netherlands Cancer Institute, Amsterdam) for providing the Mdr1a/1b;Bcrp$^{(-/-;-/-)}$ mice and the MDCKII transfected cells. Statistical analyses were kindly performed by Dr. Marcel Debray. The English text was edited by Dr. Owen Parkes. The authors declare that they have no conflict of interest.

REFERENCES

1. Scherrmann J-M. Transporters in absorption, distribution, and elimination. Chem Biodivers. 2009;6(11):1933–42.
2. Pike VW. PET radiotracers: crossing the blood–brain barrier and surviving metabolism. Trends Pharmacol Sci. 2009;30(8):431–40.
3. Abbott NJ, Patabendige AAK, Dolman DEM, Yusof SR, Begley DJ. Structure and function of the blood–brain barrier. Neurobiol Dis. 2010;37(1):13–25.
4. Tournier N, Declèves X, Saubaméa B, Scherrmann J-M, Cisternino S. Opioid transport by ATP-binding cassette transporters at the blood–brain barrier: implications for neuropsychopharmacology. Curr Pharm Des. 2011;17(26):2829–42.
5. Bartels AL. Blood–brain barrier P-glycoprotein function in neurodegenerative disease. Curr Pharm Des. 2011;17(26):2771–7.
6. Aronica E, Sisodiya SM, Gorter JA. Cerebral expression of drug transporters in epilepsy. Adv Drug Deliv Rev. 2011 [Epub ahead of print].
7. van Assema DME, Lubberink M, Bauer M, van der Flier WM, Schuit RC, Windhorst AD, *et al.* Blood–brain barrier P-glycoprotein function in Alzheimer's disease. Brain. 2011; [Epub ahead of print].
8. Hall MD, Pike VW. Avoiding barriers to PET radioligand development: cellular assays of brain efflux transporters. J Nucl Med. 2011;52(3):338–40.
9. Giacomini KM, Huang S-M, Tweedie DJ, Benet LZ, Brouwer KLR, Chu X, *et al.* Membrane transporters in drug development. Nat Rev Drug Discov. 2010;9(3):215–36.
10. Wooten DW, Moraino JD, Hillmer AT, Engle JW, Dejesus OJ, Murali D, *et al. In vivo* kinetics of [F-18]MEFWAY: a comparison with [C-11]WAY100635 and [F-18]MPPF in the nonhuman primate. Synapse. 2011;65(7):592–600.
11. Laćan G, Plenevaux A, Rubins DJ, Way BM, Defraiteur C, Lemaire C, *et al.* Cyclosporine, a P-glycoprotein modulator, increases [18F]MPPF uptake in rat brain and peripheral tissues: microPET and ex vivo studies. Eur J Nucl Med Mol Imaging. 2008;35(12):2256–66.
12. Passchier J, van Waarde A, Doze P, Elsinga PH, Vaalburg W. Influence of P-glycoprotein on brain uptake of [18F]MPPF in rats. Eur J Pharmacol. 2000;407(3):273–80.
13. la Fougère C, Böning G, Bartmann H, Wängler B, Nowak S, Just T, *et al.* Uptake and binding of the serotonin 5-HT1A antagonist [18F]-MPPF in brain of rats: effects of the novel P-glycoprotein inhibitor tariquidar. Neuroimage. 2010;49(2):1406–15.
14. Bartmann H, Fuest C, la Fougere C, Xiong G, Just T, Schlichtiger J, *et al.* Imaging of P-glycoprotein-mediated pharmacoresistance in the hippocampus: proof-of-concept in a chronic rat model of temporal lobe epilepsy. Epilepsia. 2010;51(9):1780–90.
15. Ishiwata K, Kawamura K, Yanai K, Hendrikse NH. *In vivo* evaluation of P-glycoprotein modulation of 8 PET radioligands used clinically. J Nucl Med. 2007;48(1):81–7.
16. Elsinga PH, Hendrikse NH, Bart J, van Waarde A, Vaalburg W. Positron emission tomography studies on binding of central nervous system drugs and P-glycoprotein function in the rodent brain. Mol Imaging Biol. 2005;7(1):37–44.
17. Hammers A, Bouvard S, Costes N, PereiradeSouza N, Keihaninejad S, Le Bars D, *et al.* Impact of P-glycoprotein on the distribution of [18F]-MPPF in pharmacoresistant temporal lobe epilepsia [abstract]. Epilepsia. 2010;51(Suppl):48.
18. Tournier N, Valette H, Peyronneau M-A, Saba W, Goutal S, Kuhnast B, *et al.* Transport of selected PET radiotracers by human P-glycoprotein (ABCB1) and breast cancer resistance protein (ABCG2): an *in vitro* screening. J Nucl Med. 2011;52(3):415–23.
19. Takeuchi T, Yoshitomi S, Higuchi T, Ikemoto K, Niwa S, Ebihara T, *et al.* Establishment and characterization of the transformants stably-expressing MDR1 derived from various animal species in LLC-PK1. Pharm Res. 2006;23(7):1460–72.
20. Zolnerciks JK, Booth-Genthe CL, Gupta A, Harris J, Unadkat JD. Substrate- and species-dependent inhibition of p-glycoprotein-mediated transport: Implications for predicting *in vivo* drug interactions. J Pharm Sci. 2011; [Epub ahead of print].
21. Le Bars D, Lemaire C, Ginovart N, Plenevaux A, Aerts J, Brihaye C, *et al.* High-yield radiosynthesis and preliminary *in vivo* evaluation of p-[18F]MPPF, a fluoro analog of WAY-100635. Nucl Med Biol. 1998;25(4):343–50.
22. Valette H, Xiao Y, Peyronneau M-A, Damont A, Kozikowski AP, Wei Z-L, *et al.* 18F-ZW-104: a new radioligand for imaging neuronal nicotinic acetylcholine receptors–*in vitro* binding properties and PET studies in baboons. J Nucl Med. 2009;50(8):1349–55.
23. Logan J, Fowler JS, Volkow ND, Wolf AP, Dewey SL, Schlyer DJ, *et al.* Graphical analysis of reversible radioligand binding from time-activity measurements applied to [N-11C-methyl]-(−)-cocaine PET studies in human subjects. J Cereb Blood Flow Metab. 1990;10(5):740–7.
24. Luna-Tortos C, Fedrowitz M, Loscher W. Several major antiepileptic drugs are substrates for human P-glycoprotein. Neuropharmacology. 2008;55(8):1364–75.
25. Cattelotte J, André P, Ouellet M, Bourasset F, Scherrmann J-M, Cisternino S. *In situ* mouse carotid perfusion model: glucose and cholesterol transport in the eye and brain. J Cereb Blood Flow Metab. 2008;28(8):1449–59.
26. Aznavour N, Zimmer L. [18F]MPPF as a tool for the *in vivo* imaging of 5-HT1A receptors in animal and human brain. Neuropharmacology. 2007;52(3):695–707.
27. Eyal S, Chung FS, Muzi M, Link JM, Mankoff DA, Kaddoumi A, *et al.* Simultaneous PET imaging of P-glycoprotein inhibition in multiple tissues in the pregnant nonhuman primate. J Nucl Med. 2009;50(5):798–806.
28. Wacher VJ, Silverman JA, Zhang Y, Benet LZ. Role of P-glycoprotein and cytochrome P450 3A in limiting oral absorption of peptides and peptidomimetics. J Pharm Sci. 1998;87(11):1322–30.
29. Ma Y, Lang L, Kiesewetter DO, Eckelman WC. Liquid chromatography-tandem mass spectrometry identification of metabolites of three phenylcarboxyl derivatives of the 5-HT(1A) antagonist, N-(2-(4-(2-methoxyphenyl)-1-piperazinyl)ethyl)-N-(2-pyridyl) trans-4-fluorocyclohexanecarboxamide (FCWAY), produced by human and rat hepatocytes. J Chromatogr B Analyt Technol Biomed Life Sci. 2002;780(1):99–110.
30. Thomas H, Coley HM. Overcoming multidrug resistance in cancer: an update on the clinical strategy of inhibiting p-glycoprotein. Cancer Control. 2003;10(2):159–65.
31. Carson RE, Wu Y, Lang L, Ma Y, Der MG, Herscovitch P, *et al.* Brain uptake of the acid metabolites of F-18-labeled WAY 100635 analogs. J Cereb Blood Flow Metab. 2003;23(2):249–60.

32. Plenevaux A, Weissmann D, Aerts J, Lemaire C, Brihaye C, Degueldre C, *et al.* Tissue distribution, autoradiography, and metabolism of 4-(2′-methoxyphenyl)-1-[2′ -[N-2″-pyridinyl)-p-[(18)F] fluorobenzamido]ethyl]piperazine (p-[(18)F]MPPF), a new serotonin 5-HT(1A) antagonist for positron emission tomography: an *in vivo* study in rats. J Neurochem. 2000;75(2):803–11.
33. Lang L, Jagoda E, Schmall B, Vuong BK, Adams HR, Nelson DL, *et al.* Development of fluorine-18-labeled 5-HT1A antagonists. J Med Chem. 1999;42(9):1576–86.
34. Costes N, Merlet I, Zimmer L, Lavenne F, Cinotti L, Delforge J, *et al.* Modeling [18-F]MPPF positron emission tomography kinetics for the determination of 5-hydroxytryptamine(1A) receptor concentration with multiinjection. J Cereb Blood Flow Metab. 2002;22(6):753–65.
35. Passchier J, van Waarde A, Vaalburg W, Willemsen AT. On the quantification of [18F]MPPF binding to 5-HT1A receptors in the human brain. J Nucl Med. 2001;42(7):1025–31.
36. Tournier N, Chevillard L, Megarbane B, Pirnay S, Scherrmann J-M, Declèves X. Interaction of drugs of abuse and maintenance treatments with human P-glycoprotein (ABCB1) and breast cancer resistance protein (ABCG2). Int J Neuropsychopharmacol. 2010;13(7):905–15.
37. Zhang C, Zuo Z, Kwan P, Baum L. *In vitro* transport profile of carbamazepine, oxcarbazepine, eslicarbazepine acetate, and their active metabolites by human P-glycoprotein. Epilepsia. 2011;52 (10):1894–904.
38. Mandula H, Parepally JM, Feng R, Smith QR. Role of site-specific binding to plasma albumin in drug availability to brain. J Pharmacol Exp Ther. 2006;317(2):667–75.
39. Passchier J, van Waarde A, Pieterman RM, Elsinga PH, Pruim J, Hendrikse HN, *et al. In vivo* delineation of 5-HT1A receptors in human brain with [18F]MPPF. J Nucl Med. 2000;41(11):1830–5.
40. Toffoli G, Aita P, Sorio R, Corona G, Bertola A, Colussi AM, *et al.* Effect of cyclosporin A on protein binding of teniposide in cancer patients. Anticancer Drugs. 1999;10(6):511–8.
41. Liow JS, Lu S, McCarron JA, Hong J, Musachio JL, Pike VW, *et al.* Effect of a P-glycoprotein inhibitor, Cyclosporin A, on the disposition in rodent brain and blood of the 5-HT1A receptor radioligand, [11C](R)-(−)-RWAY. Synapse. 2007;61(2):96–105.
42. Yasuno F, Zoghbi SS, McCarron JA, Hong J, Ichise M, Brown AK, *et al.* Quantification of serotonin 5-HT1A receptors in monkey brain with [11C](R)-(−)-RWAY. Synapse. 2006;60(7):510–20.
43. Syvänen S, Lindhe O, Palner M, Kornum BR, Rahman O, Langström B, *et al.* Species differences in blood–brain barrier transport of three positron emission tomography radioligands with emphasis on P-glycoprotein transport. Drug Metab Dispos. 2009;37(3):635–43.
44. Zoghbi SS, Liow JS, Yasuno F, Hong J, Tuan E, Lazarova N, *et al.* 11C-loperamide and its N-desmethyl radiometabolite are avid substrates for brain permeability-glycoprotein efflux. J Nucl Med. 2008;49(4):649–56.